



## **Thermal Analysis of an M256 120-mm Cannon**

**by Joseph T. South and Robert H. Carter**

**ARL-TR-3594**

**August 2005**

## **NOTICES**

### **Disclaimers**

The findings in this report are not to be construed as an official Department of the Army position unless so designated by other authorized documents.

Citation of manufacturer's or trade names does not constitute an official endorsement or approval of the use thereof.

**DESTRUCTION NOTICE**—Destroy this report when it is no longer needed. Do not return it to the originator.

# **Army Research Laboratory**

Aberdeen Proving Ground, MD 21005-5069

---

**ARL-TR-3594****August 2005**

---

## **Thermal Analysis of an M256 120-mm Cannon**

**Joseph T. South and Robert H. Carter**  
**Weapons and Materials Research Directorate, ARL**

REPORT DOCUMENTATION PAGE				Form Approved OMB No. 0704-0188	
<p>Public reporting burden for this collection of information is estimated to average 1 hour per response, including the time for reviewing instructions, searching existing data sources, gathering and maintaining the data needed, and completing and reviewing the collection information. Send comments regarding this burden estimate or any other aspect of this collection of information, including suggestions for reducing the burden, to Department of Defense, Washington Headquarters Services, Directorate for Information Operations and Reports (0704-0188), 1215 Jefferson Davis Highway, Suite 1204, Arlington, VA 22202-4302. Respondents should be aware that notwithstanding any other provision of law, no person shall be subject to any penalty for failing to comply with a collection of information if it does not display a currently valid OMB control number.</p> <p><b>PLEASE DO NOT RETURN YOUR FORM TO THE ABOVE ADDRESS.</b></p>					
1. REPORT DATE (DD-MM-YYYY) August 2005		2. REPORT TYPE Final		3. DATES COVERED (From - To) November 2003 to May 2004	
4. TITLE AND SUBTITLE  Thermal Analysis of an M256 120-mm Cannon				5a. CONTRACT NUMBER	
				5b. GRANT NUMBER	
				5c. PROGRAM ELEMENT NUMBER	
6. AUTHOR(S)  Joseph T. South and Robert H. Carter (both of ARL)				5d. PROJECT NUMBER 622618.H80	
				5e. TASK NUMBER	
				5f. WORK UNIT NUMBER	
7. PERFORMING ORGANIZATION NAME(S) AND ADDRESS(ES) U.S. Army Research Laboratory Weapons and Materials Research Directorate Aberdeen Proving Ground, MD 21005-5069				8. PERFORMING ORGANIZATION REPORT NUMBER  ARL-TR-3594	
9. SPONSORING/MONITORING AGENCY NAME(S) AND ADDRESS(ES)				10. SPONSOR/MONITOR'S ACRONYM(S)	
				11. SPONSOR/MONITOR'S REPORT NUMBER(S)	
12. DISTRIBUTION/AVAILABILITY STATEMENT Approved for public release; distribution is unlimited.					
13. SUPPLEMENTARY NOTES					
14. ABSTRACT  In this work, the development and verification of a thermal finite element model for the M256 120-mm cannon is reported. Surface and interior temperatures of the M256 at various times and locations are reported after being subjected to a simulated ballistic event. This report details the development of the models with emphasis on mesh refinement for improved fidelity. The results of the model agree with experimentally obtained M256 thermal data.					
15. SUBJECT TERMS 120-mm cannon; FEA; finite element analysis; M256; thermal					
16. SECURITY CLASSIFICATION OF:			17. LIMITATION OF ABSTRACT  SAR	18. NUMBER OF PAGES  25	19a. NAME OF RESPONSIBLE PERSON Joseph T. South
a. REPORT Unclassified	b. ABSTRACT Unclassified	c. THIS PAGE Unclassified			19b. TELEPHONE NUMBER (Include area code) 410-306-0763

---

## Contents

---

<b>List of Figures</b>	<b>iv</b>
<b>List of Tables</b>	<b>iv</b>
<b>1. Introduction</b>	<b>1</b>
<b>2. Approach</b>	<b>2</b>
<b>3. Input and Model Generation</b>	<b>2</b>
3.1 Mesh Sensitivity Analysis .....	4
<b>4. Results</b>	<b>7</b>
4.1 ID Temperature Results.....	7
4.2 Sub-surfaceTemperature Results.....	8
<b>5. Summary</b>	<b>12</b>
<b>6. References</b>	<b>13</b>
<b>Distribution List</b>	<b>14</b>

---

## List of Figures

---

Figure 1. Heat flux of the propellant gas as a function of time and axial location.....	3
Figure 2. Cross section of the graded mesh density.....	4
Figure 3. Results of the mesh sensitivity analysis .....	5
Figure 4. Through thickness temperature profiles at 640 mm from the RFT and 4.5 ms for a 120-mm steel barrel with varying mesh densities.....	5
Figure 5. The effect of the number of elements on solution time and ID temperature.....	6
Figure 6. Predicted ID temperatures as a function of time at the four axial locations.....	7
Figure 7. Predicted ID temperature at 640 mm from the RFT compared to the predicted temperature of Conroy et al. ....	8
Figure 8. Sub-surface model prediction at 640 mm from the RFT compared to experimental measurements.....	9
Figure 9. Sub-surface model prediction at 1050 mm from the RFT compared to experimental measurements.....	9
Figure 10. Sub-surface model prediction at 1350 mm from the RFT compared to experimental measurements.....	10
Figure 11. Sub-surface model prediction at 1600 mm from the RFT compared to experimental measurements.....	10
Figure 12. Sub-surface model prediction at 640 mm from the RFT showing the perturbation that occurs near the ID. ....	12

---

## List of Tables

---

Table 1. Steel thermal properties used in the finite element model.....	2
---	---

---

## 1. Introduction

---

In this research, a two-dimensional (2-D) axisymmetric, transient, thermal finite element model of an M256 120-mm cannon has been generated. The goal of the research was to develop and validate a method to determine the surface and interior temperatures of an M256 at any time and location after it is subjected to a ballistic event. Previous thermal analyses of the M256 cannon have been performed; however, these investigations did not have the ability to continuously evaluate the temperatures within the cannon walls as function of time ( $t$ ).

The motivation for this research has been the development of advanced multi-material weapon systems. Advanced weapons systems for the Future Combat System may consist of hybrid barrels enabling these systems to achieve a lower combat load as well as offering the potential for increased muzzle velocity. The development of advanced gun systems requires a design that is robust mechanically as well as thermally. Mechanical strength is required so that the system will survive the ballistic event, and thermal stability is required so that the hybrid system does not deform or lose its mechanical integrity because of ballistic heating.

D'Andrea et al. (2) found that the success of ceramic liners in cannon barrels resides in the controlling of longitudinal residual stresses, thermal gradients at the material interfaces, and the effects of differing coefficients of thermal expansion. They concluded that for a hybrid multi-material weapon system to survive the ballistic event, a multi-axial constraint is necessary. This multi-axial constraint can be realized when the barrel liner is sheathed in such a way as to induce a compressive pre-stress. This sheath can be either a metallic or an organic based composite system. The temperature profile and thermal stresses become important because of the dissimilar materials of the liner and sheath. In the case of an organic based sheathing system, the temperature of the liner-sheath interface becomes paramount to the performance of the system because of the low operating temperature limits of the polymeric matrix materials. Knowledge of the temperature profile is essential for the stress states to be designed at the interface since they must remain in compression at all times. Given the extremely high flame temperatures of large caliber propellants, it is imperative that an approach be developed that would allow for the prediction of the axial as well as the radial temperature profiles.

Before the finite element method is used to calculate the temperature profile for multi-material system, the models need to be developed and verified on all steel configurations. This will allow for observation of the effects of the different analytical parameters such as mesh density on the calculated temperature profile.

---

## 2. Approach

---

The finite element approach was chosen to evaluate the surface and interior temperature of an M256. The barrel dimensions were obtained from the specified technical drawings (3). Because of the nature of the problem, symmetry was employed to reduce the model from a three-dimensional analysis to a 2-D axisymmetric analysis. A 2-D axisymmetric sketch of the barrel was created in a computer-aided drawing package (CAD) and then exported into the ANSYS<sup>1</sup> finite element software. The use of this symmetric condition allowed for more economical computation time.

---

## 3. Input and Model Generation

---

In order to perform the analysis, the model required the material input over a range of temperatures. The thermal properties required were density, specific heat, and thermal conductivity. The steel thermal properties employed in the model are listed in table 1 (4). The material property data were limited to an upper temperature of 1143 K. If a material property was required at a higher temperature, the finite element software performed an extrapolation based upon table 1 to approximate the value.

Table 1. Steel thermal properties used in the finite element model.

Bulk Density (Kg m <sup>-3</sup> )	Temperature (°C)	Temperature (K)	Specific Heat C <sub>p</sub> (J kg <sup>-1</sup> K <sup>-1</sup> )	Conductivity λ(W m <sup>-1</sup> K <sup>-1</sup> )
7800	-239.55	33.45	411.69	12.28
7800	-128.59	144.41	434.18	27.58
7800	-17.64	255.36	459.03	34.89
7800	93.32	366.32	486.99	38.07
7800	204.28	477.28	515.64	38.63
7800	315.23	588.23	551.37	37.61
7800	426.19	699.19	594.63	35.87
7800	537.14	810.14	654.27	33.51
7800	648.10	921.10	730.34	30.71
7800	759.06	1032.06	1493.83	26.99
7800	870.01	1143.01	584.62	27.01

The thermal forcing input into the model was provided by Conroy et al. (5) and computed through a coupled approach of interior ballistic calculations via XKTC2 (6) as well as the U.S. Army Research Laboratory version of XBR-2D (7,8). The boundary conditions were for an M829A2

---

<sup>1</sup>ANSYS, which is not an acronym, is a registered trademark of ANSYS, Inc.



projectile fired at 294 K. Ambient temperature was assumed to be 293 K. The interior ballistic code yielded the gas velocities, gas temperatures, and pressure. These core flow data were used as input to the ARL XBR-2D heat transfer/conduction code which then generated the heat transfer coefficients, film temperatures, and heat flux for 38 points along the inner diameter (ID) of the barrel at every microsecond. The described calculation methodology also produces barrel thermal profiles for arbitrary firing scenarios. The total time of the thermal forcing input was 0.9 second. A plot of the heat flux as a function of axial location and time is shown in figure 1. The data have been reduced for the ease of presentation. In the finite element model, either the heat flux or both the gas temperature and gas heat transfer coefficients were applied to simulate the ballistic event.

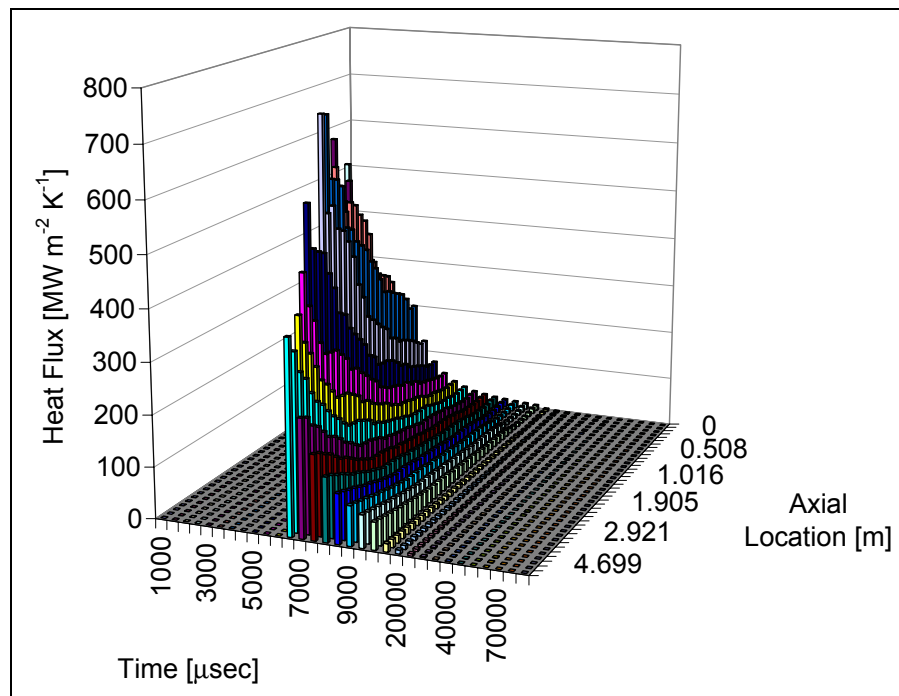


Figure 1. Heat flux of the propellant gas as a function of time and axial location.

In the finite element model, the thermal forcing input was applied to the ID of the barrel and prescribed as tabular data. This yielded a data table consisting of 342,076 points. Application of the data as a table allowed for linear interpolation of the thermal data between the 38 known values along the ID. This linear interpolation, which was performed within the simulation, produced a smooth application of the input data during the analysis. To simulate operation of the cannon on an average day, thermal boundary conditions, constant heat transfer coefficient of  $11.45 \text{ W/m}^2$ , and a temperature of 293 K were placed on the outer diameter (OD) of the cannon.

The next step in the model generation was meshing of the barrel. The barrel was meshed with 2-D axisymmetric eight-node elements. Higher order elements were used since the underlying quadratic shape function to the element is able to more accurately represent the results attributable to the ballistic event. The barrel was meshed with an element gradient that decreased in mesh density through the thickness from the ID to the OD. A cross-sectional view of this

gradient is presented as figure 2. The purpose of the element gradient was to reduce the overall number of elements as the highly refined mesh was only required on the ID of the barrel where the combustion gases acted.

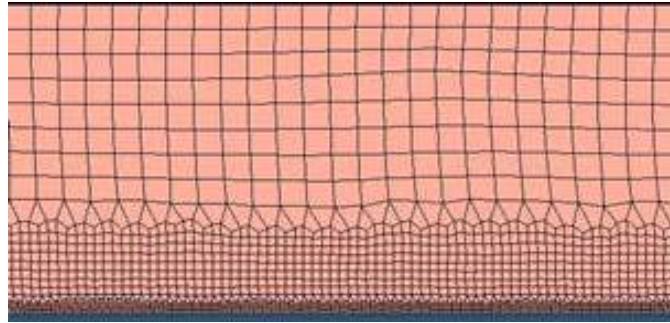


Figure 2. Cross section of the graded mesh density. (The ID is at the bottom, the OD is on the top.)

### 3.1 Mesh Sensitivity Analysis

When the basic model was constructed, a mesh sensitivity analysis was performed to determine the optimum element size along the ID to yield accurate results. Four different variations of the model were created: coarse, medium, fine, and very fine. The coarse model has a base element size of 5 mm. In each of the following models, the elements along the ID of the barrel were refined to reduce their size. The very fine model possessed a final element size of 47  $\mu\text{m}$ , providing an order of magnitude reduction in element size compared to the coarse model.

The results of the mesh sensitivity analysis are presented in figures 3 through 5. Figure 3 shows the ID temperature at 640 mm from the rear face of the tube (RFT). The element size has a pronounced effect on the maximum predicted ID temperature. Increasing the mesh density greatly increases the predicted ID temperature. Both the coarse and the medium mesh density models appear to greatly under-predict the temperature at the ID, while the fine and the very fine models predict nearly the same temperature. An important feature to note is the fast rise of the temperature because of the ballistic event and the subsequent reduction of the temperature as the event passes and thermal energy can be diffused into the bulk of the barrel.

The effect of the mesh density on the “through-thickness” temperature is plotted in figure 4. The figure shows the temperature through the thickness at 640 mm the RFT at 4.5 ms. The mesh density greatly affects the shape of the results. The figure shows a polynomial dependence of the temperature from the ID to the OD. This result is attributable to the quadratic shaped function of the eight-node element. The flux from the ballistic event, as shown in figure 1, is large enough and occurs over a small time period so that it places an extremely large  $\Delta T$  across the element on the ID. The response of the element is limited to a quadratic shape function, which is not able to accurately represent the temperature profile. For a coarse mesh density, the quadratic element results in a response that over-predicts and then under-predicts the response of the system before reaching thermal equilibrium far from the ID. The magnitude and depth of this resulting error

depend on the element size, and both are reduced as the element size is decreased. With a higher mesh density near the ID, the gradient is divided into sections that can be better represented by the quadratic shape function. The result is that the solution becomes more uniform; however, there are still minor deviations for the fine and very fine results.

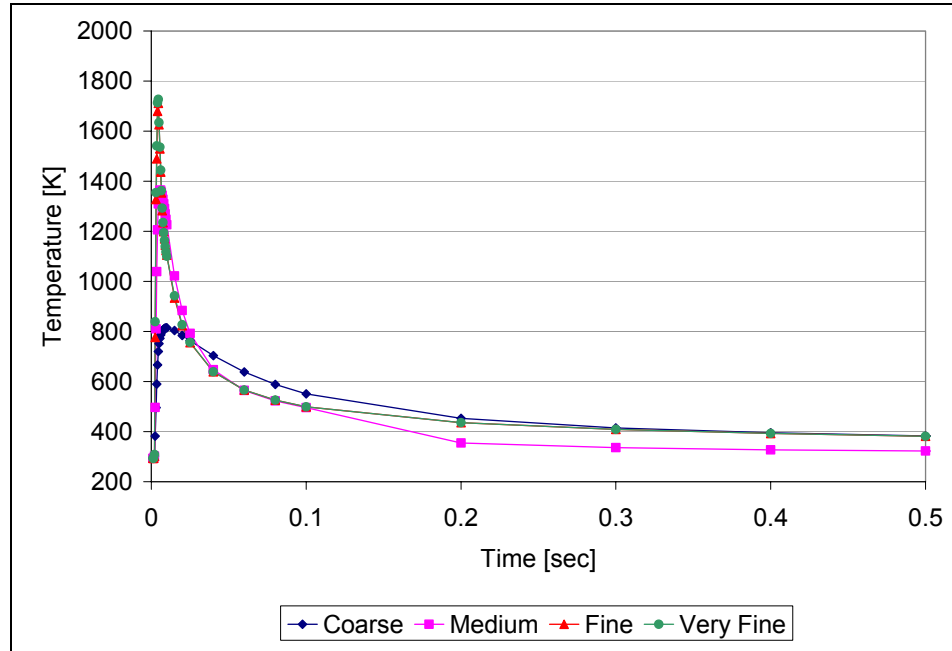


Figure 3. Results of the mesh sensitivity analysis (ID temperature profiles at 640 mm RFT for a 120-mm steel barrel with varying mesh densities).

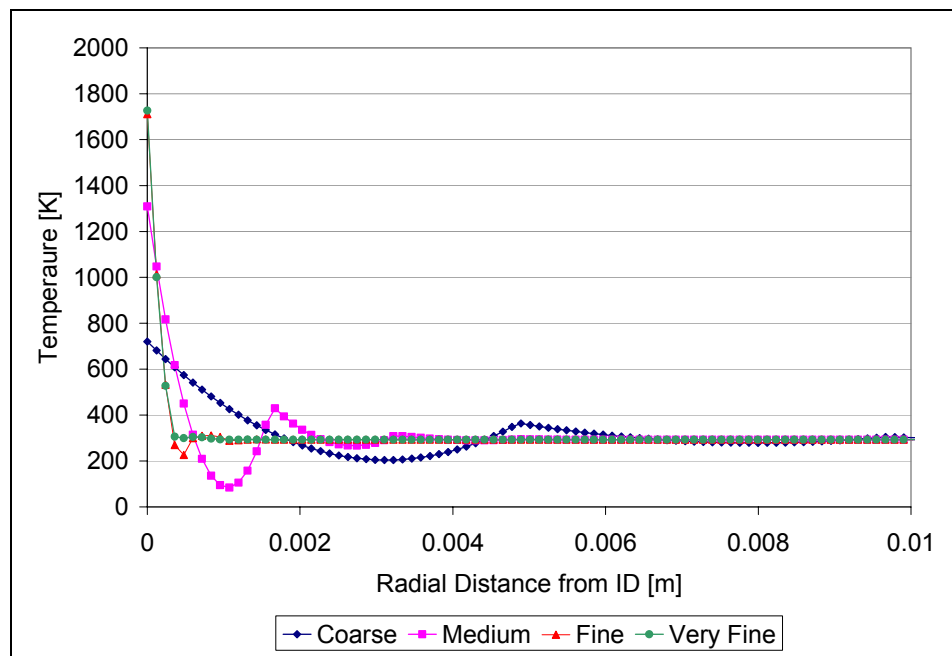


Figure 4. Through thickness temperature profiles at 640 mm from the RFT and 4.5 ms for a 120-mm steel barrel with varying mesh densities.

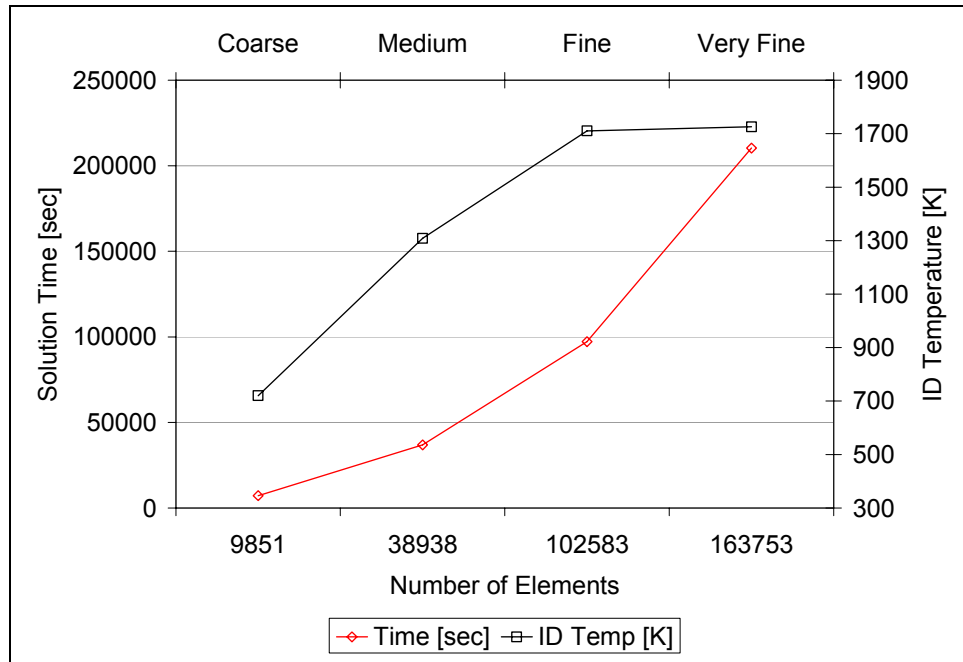


Figure 5. The effect of the number of elements on solution time and ID temperature.

The mesh density greatly affects the results on the ID as well as through the thickness. Increasing the mesh density can improve the results but at the expense of computation time. Figure 5 presents the effect of the number of elements on solution time and ID temperature. It is seen in the figure that there is very little difference between the predicted ID temperatures of the fine and very fine models; however, the solution time between the two differs by almost a factor of two.

The areas of the model were meshed with the plane 82 ANSYS element. This is an eight-noded 2-D element with plasticity and axisymmetric capability. The axis of symmetry was the y-axis.

The results of the mesh sensitivity analysis showed that the results of the thermal model are highly dependent upon the element size for the ID as well as through the thickness. Because of the high heat flux that is placed on the barrel during the ballistic event, the first element on the ID of the barrel experiences a large  $\Delta T$ . This large  $\Delta T$  is similar to a step load. The model must use the underlying element shape function to achieve convergence. This produces both an under-prediction of the ID temperature and a quadratic dependence through the thickness of the model. Increasing the mesh density will reduce these effects but at the expense of solution time. Very fine element densities are appropriate for one-shot thermal models that require high fidelity; however, for models that require multiple shots or bulk material response, a fine element density would suffice.

---

## 4. Results

---

The model results were evaluated and compared to the experimental and predicted work of Conroy et al. (6-7). The primary goal was to validate the modeling methodology and approach. For this reason, the results of the very fine model were used since they produced the highest fidelity of the four models analyzed. Results of the model produced temperature, thermal gradients, and thermal fluxes as functions of both time and location. The model results were examined at four different axial locations: 640, 1050, 1350, and 1600 mm from the RFT. These locations were chosen so that the model results could be compared with the results of Conroy et al. (6-7) generated with the XBR2D-V29 code.

### 4.1 ID Temperature Results

The model predictions at the four axial locations as a function of time are presented in figure 6. Included in the figure is the predicted ID temperature at 640 mm from the RFT from Conroy et al. There are several features to note in the figure. First is that the highest ID temperatures occur at 640 mm from the RFT. Peak temperatures decrease as axial location moves toward the muzzle. A second feature to note is that all the ID temperatures exhibit an exponential decay with time.

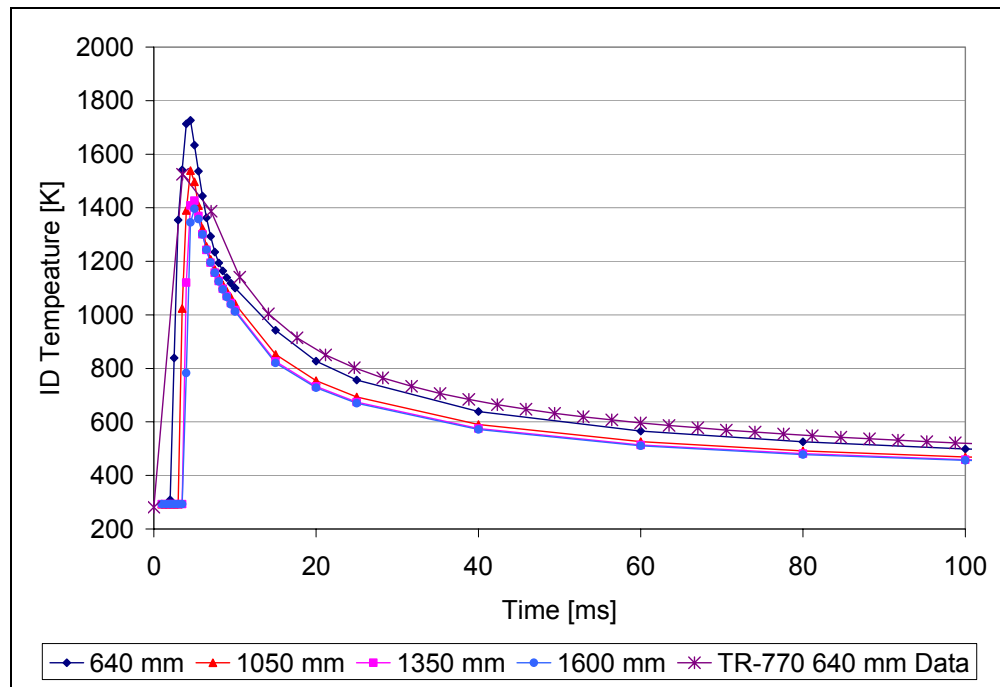


Figure 6. Predicted ID temperatures as a function of time at the four axial locations. (Included in the figure are the predicted data of Conroy et al.)

An interesting result from the prediction is the difference in both the shape of the 640-mm RFT curve and the peak temperature compared to the data of Conroy et al. Figure 7 is a plot of only the data at 640 mm from the RFT. Both curves in the figure demonstrate roughly the same rise and fall after peak temperature, but there is a predicted difference for the peak temperature. The finite element analysis (FEA) model predicts a peak temperature of 1726 K, while the XBR2D-V29 code predicts a peak of 1524 K. It appears that the difference may be attributable to a sampling error. The FEA predictions possess five points between the times of 3.5 and 6.5 ms, while none were output from the XBR2D-V29 code. The difference may also be because the FEA model did not include a chrome coating in the ID. The inclusion of the chrome, which possesses a higher thermal conductivity of  $84 \text{ W m}^{-1} \text{ K}^{-1}$  than steel would slightly reduce the ID temperature by being able to transport more thermal energy to the bulk material. However, with a chrome thickness of  $140 \text{ }\mu\text{m}$ , it is unlikely that the 200-K  $\Delta T$  between the two models could be overcome. The difference between the two models is most likely attributable to the sampling rate. Regardless, the FEA model does appear to accurately predict the thermal response at the ID of the system.

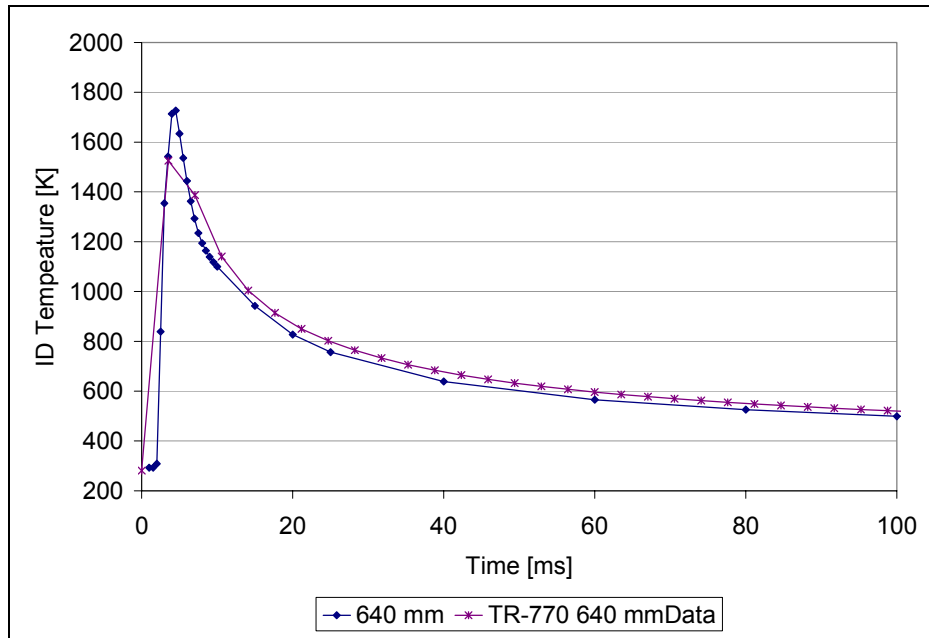


Figure 7. Predicted ID temperature at 640 mm from the RFT compared to the predicted temperature of Conroy et al.

## 4.2 Sub-surface Temperature Results

To continue the validation of the model, the predicted sub-surface temperatures were compared to experimental data. In Conroy et al., an M256 gun tube was instrumented with in-wall thermocouples at the axial locations of 640, 1050, 1350, and 1600 mm from the RFT. The probes were ideally 1.27 mm from the bore surface. The results of the sub-surface analysis are presented as figures 8 through 11. The original experimental data for the figures possessed baseline temperatures between 280 and 283 K. In order to conduct an accurate comparison with

the model results, the experimental data were increased to have a baseline temperature of 293 K. For each experimental axial location, five different radial model predictions were made. The exact radial locations vary slightly between the four axial locations since the model results can only be supplied where there is a node present in the finite element model.

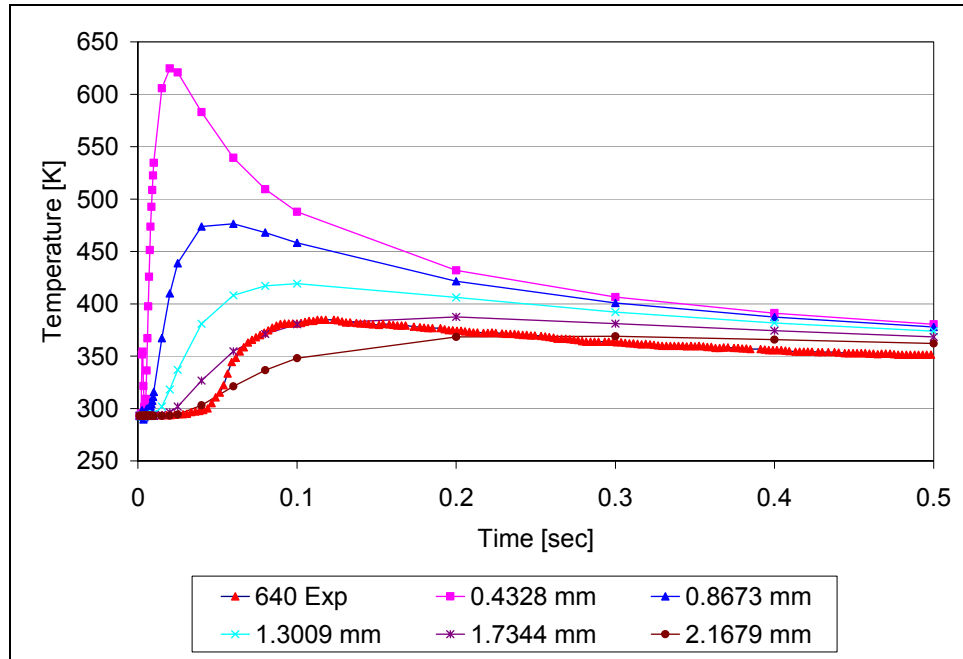


Figure 8. Sub-surface model prediction at 640 mm from the RFT compared to experimental measurements.

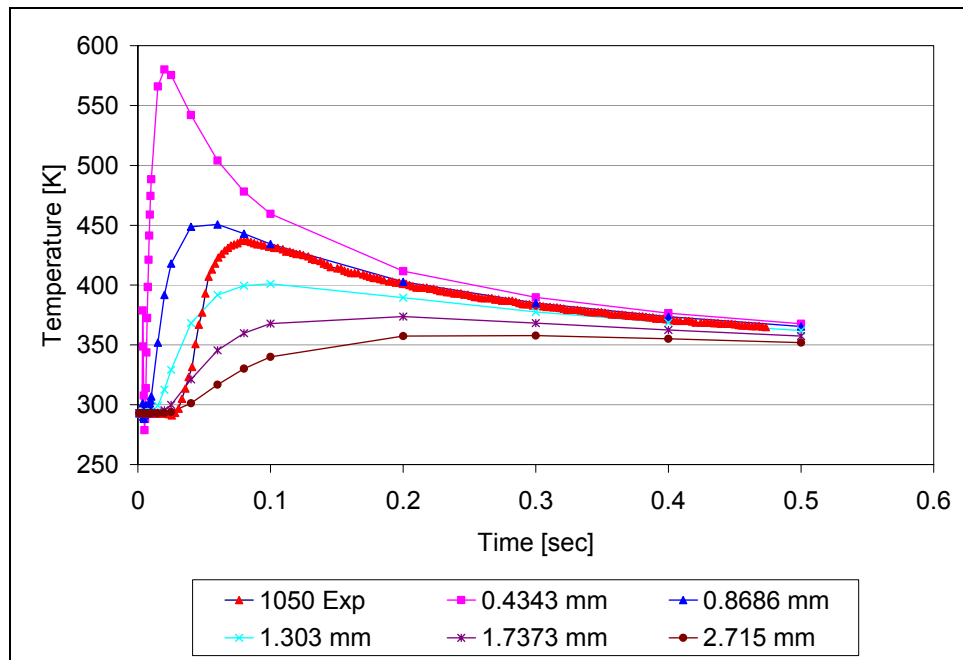


Figure 9. Sub-surface model prediction at 1050 mm from the RFT compared to experimental measurements.

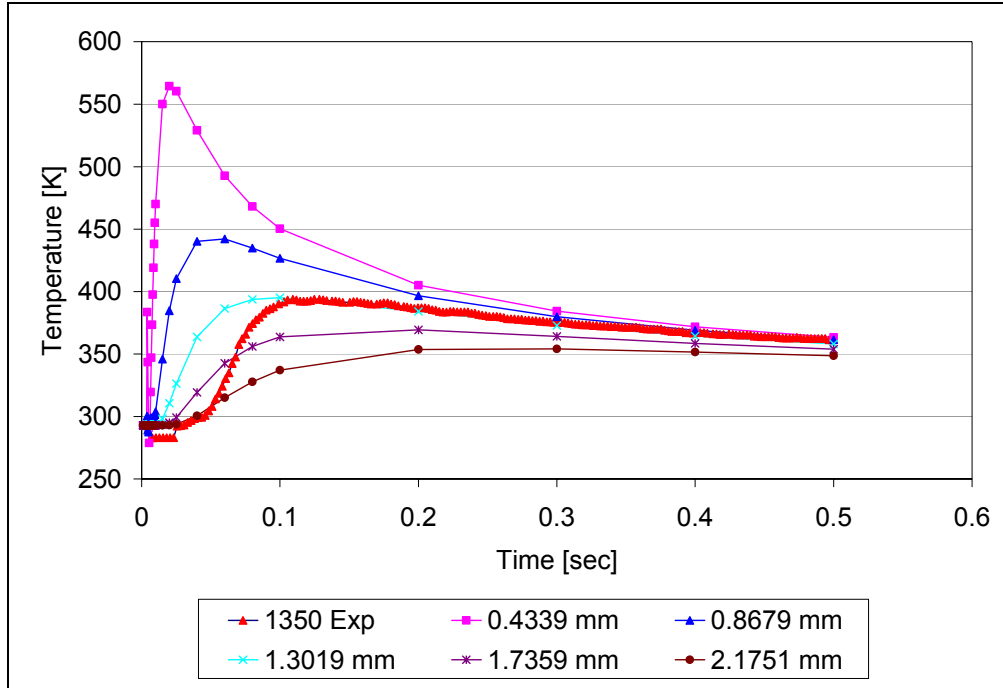


Figure 10. Sub-surface model prediction at 1350 mm from the RFT compared to experimental measurements.

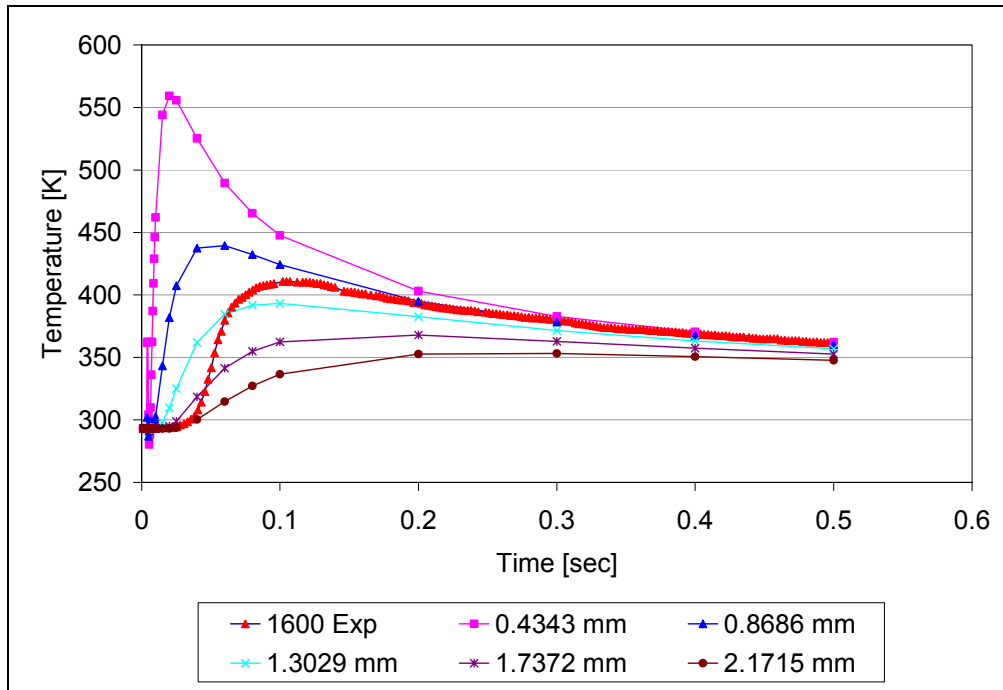


Figure 11. Sub-surface model prediction at 1600 mm from the RFT compared to experimental measurements.

Figure 8 presents the sub-surface model predictions compared to the experimental thermocouple data. The experimental data best match the prediction at 1.7344 mm. This value falls within the



range predicted by Conroy et al., who found the experimental data lying between 1.52 and 1.78 mm. In their calculations, the experimental data were closer to the 1.52-mm prediction while the FEA prediction best matches the 1.7344-mm point. Given that their model predicted a lower ID temperature than the FEA, it makes sense that the FEA would predict the same temperature farther from the ID surface. In figure 8, the predicted and the experimental data do not asymptotically approach one another as time increases. This result was also found in Conroy et al. Most likely, the difference between the experimental and the predicted was attributable to the error associated with the thermocouple.

There appears to be a delay of approximately 35 ms between the experimental and the predicted results. If data were shifted, by this time there would be closer agreement between the two data sets. It is believed that the difference in the time may be attributable to an overly simplistic model of the ignition delay and the flame spreading process. Although this research used a modern interior ballistics code, the physics of the codes have not changed but the fidelity has increased dramatically. The temporal disparities attributable to ignition and flame spreading are an intrinsic feature of interior ballistics codes (8).

The results for the axial 1050, 1350, and 1600 mm from the RFT locations, shown in figures 9 through 11, demonstrate similar behavior as the 640 mm from the RFT point. These temperatures versus time plots demonstrate similar shapes and magnitudes. In all four cases, the experimental data are bound by the FEA results within 1 mm of the ideal 1.25-mm radial location. The hypothesis that the 640-mm data were affected by the thermocouple is supported as the data asymptotically approach a steady state value for the 1050-, 1350-, and 1600-mm locations.

A feature to note in figures 8 through 11 is that a perturbation still exists close to the ID. Figure 12 shows this perturbation for the 640-mm axial location. As discussed in the mesh sensitivity analysis section, the elements in the FEA have an underlying quadratic shape function. Despite the 47- $\mu\text{m}$  size of the ID elements, the heat flux from the ballistic event is so great that a minor perturbation of the results can still occur through the thickness. The magnitude of this perturbation will approach 0 as the element size decreases; this was shown in figure 4.

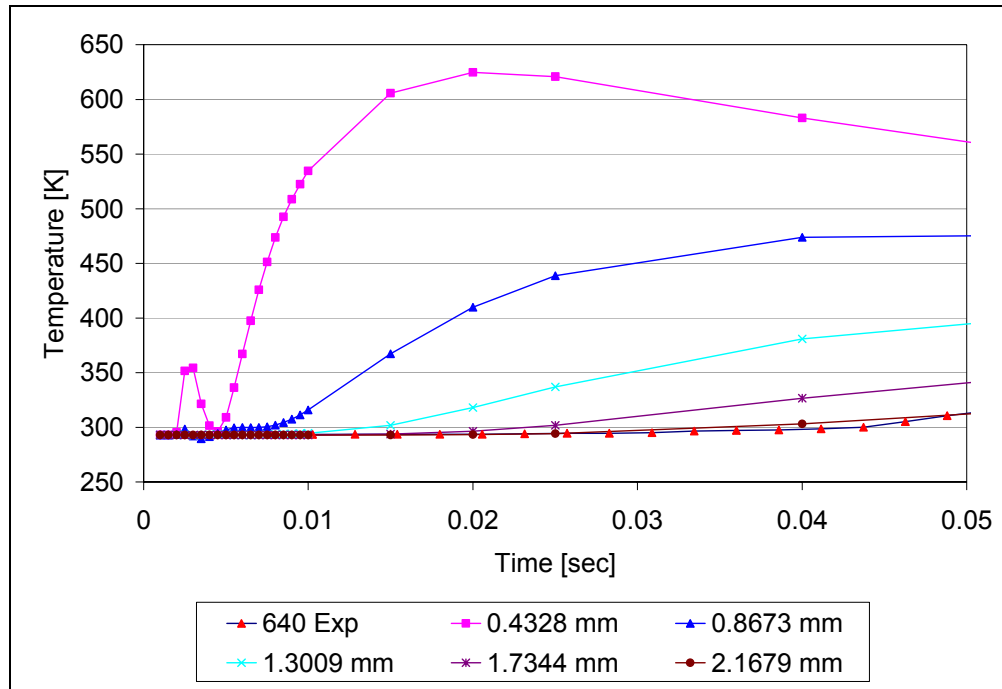


Figure 12. Sub-surface model prediction at 640 mm from the RFT showing the perturbation that occurs near the ID.

---

## 5. Summary

---

FEA is capable of calculating the thermal profiles for an M256 cannon. Mesh density is important for accuracy and to minimize anomalous behavior because of interpolation errors attributable to large gradients across a single element. The cost of accuracy versus computation time is demonstrated as the ID temperature appears to asymptotically approach a value at the expense of computation time. When compared to previous analyses, the data appear to be very similar. The temperatures are accurate within a millimeter of the stated position of the thermocouple when compared to experimental test data. These results support using this modeling approach to calculate the temperature profiles for hybrid barrel designs.

---

## 6. References

---

1. Artus B.; Hasenbein R. *Thermal Study of the 120-mm M256 Cannon Tube*; TR ARCCB-TB-89028; U.S. ARDEC, 1989.
2. D'Andrea G.; Cullinan R. L.; Croteau P. J. *Refractory-Lined Composite Pressure Vessels*; Technical Report ARLCB-TR-78023; U.S. Army Research and Development Command: Watervliet, NY, 1978.
3. M256 Technical Data Package, Armament Research Development and Engineering Center, Picatinny Arsenal, NJ
4. Hummel R. E. *Electronic Properties of Materials*, 2nd Ed., Springer-Verlag, New York, New York, 1993.
5. Conroy P. J.; Bundy M. L.; Kennedy J. L. *Simulated and Experimental In-Wall Temperatures for 120-mm Ammunition*; ARL-TR-770; U.S. Army Research Laboratory: Aberdeen Proving Ground, MD, 1995.
6. Gough P. S. *The XNOVAKTC Code*; BRL-CR-627; U.S. Army Ballistic Research Laboratory: Aberdeen Proving Ground, MD, 1990.
7. Conroy, P.J. *Gun Tube Heating*; BRL-TR-3300; U.S. Army Ballistic Research Laboratory: Aberdeen Proving Ground, MD, December 1991.
8. Crickenberger, A.B.; Talley, R.L.; Taller, J.Q. *Modifications to the XBR-2D Heat Conduction Code*; ARL-CR-126; U.S. Army Research Laboratory: Aberdeen Proving Ground, MD, April 2004.
9. Conroy, P. J.; Bundy, M. L.; Kennedy, J. L. Simulated and Experimental In-Wall Temperatures for 120-mm Ammunition. *Defence Science Journal* **1996**, 46 (4), 223-232.
10. Conroy P. J. personal communication, U.S. Army Research Laboratory: Aberdeen Proving Ground, MD, July 2005.

NO. OF  
COPIES ORGANIZATION

\* ADMINISTRATOR  
DEFENSE TECHNICAL INFO CTR  
ATTN DTIC OCA  
8725 JOHN J KINGMAN RD STE 0944  
FT BELVOIR VA 22060-6218  
\*pdf file only

1 DIRECTOR  
US ARMY RSCH LABORATORY  
ATTN IMNE ALC IMS MAIL & REC MGMT  
2800 POWDER MILL RD  
ADELPHI MD 20783-1197

1 DIRECTOR  
US ARMY RSCH LABORATORY  
ATTN AMSRD ARL CI OK TL TECH LIB  
2800 POWDER MILL RD  
ADELPHI MD 20783-1197

1 DIRECTOR  
US ARMY RESEARCH LAB  
ATTN AMSRD ARL SE DE R ATKINSON  
2800 POWDER MILL RD  
ADELPHI MD 20783-1197

6 DIR US ARMY RESEARCH LAB  
ATTN AMSRD ARL WM MB T LI  
A ABRAHAMIAN M BERMAN  
M CHOWDHURY A FRYDMAN  
E SZYMANSKI  
2800 POWDER MILL RD  
ADELPHI MD 20783-1197

1 COMMANDER  
US ARMY MATERIEL CMD  
ATTN AMXMI INT  
5001 EISENHOWER AVE  
ALEXANDRIA VA 22333-0001

3 PM MAS  
ATTN SFAE AMO MAS  
SFAE AMO MAS MC  
CHIEF ENGINEER  
PICATINNY ARSENAL NJ 07806-5000

2 PM MAS  
ATTN SFAE AMO MAS PS  
SFAE AMO MAS LC  
PICATINNY ARSENAL NJ 07806-5000

1 CDR US ARMY ARDEC  
ATTN AMSTA AR CC COL JENKER  
PICATINNY ARSENAL NJ 07806-5000

NO. OF  
COPIES ORGANIZATION

1 CDR US ARMY ARDEC  
ATTN AMSTA AR FSE  
PICATINNY ARSENAL NJ 07806-5000

1 CDR US ARMY ARDEC  
ATTN AMSTA AR TD  
PICATINNY ARSENAL NJ 07806-5000

7 CDR US ARMY ARDEC  
ATTN AMSTA AR CCH A D VO  
F ALTAMURA M NICOLICH  
M PALATHINGUL R HOWELL  
A VELLA M YOUNG  
PICATINNY ARSENAL NJ 07806-5000

6 CDR US ARMY ARDEC  
ATTN AMSTA AR CCH A L MANOLE  
S MUSALLI R CARR M LUCIANO  
E LOGSDEN T LOUZEIRO  
PICATINNY ARSENAL NJ 07806-5000

1 CDR US ARMY ARDEC  
ATTN AMSTA AR CCH P J LUTZ  
PICATINNY ARSENAL NJ 07806-5000

1 CDR US ARMY ARDEC  
ATTN AMSTA AR FSF T C LIVECCHIA  
PICATINNY ARSENAL NJ 07806-5000

1 CDR US ARMY ARDEC  
ATTN AMSTA ASF  
PICATINNY ARSENAL NJ 07806-5000

1 CDR US ARMY ARDEC  
ATTN AMSTA AR QAC T C J PAGE  
PICATINNY ARSENAL NJ 07806-5000

1 CDR US ARMY ARDEC  
ATTN AMSTA AR M D DEMELLA  
PICATINNY ARSENAL NJ 07806-5000

3 CDR US ARMY ARDEC  
ATTN AMSTA AR FSA A WARNASH  
B MACHAK M CHIEFA  
PICATINNY ARSENAL NJ 07806-5000

2 CDR US ARMY ARDEC  
ATTN AMSTA AR FSP G M SCHIKSNIS  
D CARLUCCI  
PICATINNY ARSENAL NJ 07806-5000

2 CDR US ARMY ARDEC  
ATTN AMSTA AR CCH C H CHANIN  
S CHICO  
PICATINNY ARSENAL NJ 07806-5000

NO. OF  
COPIES    ORGANIZATION

- 1    CDR US ARMY ARDEC  
ATTN AMSTA AR QAC T D RIGOGLIOSO  
PICATINNY ARSENAL NJ 07806-5000
- 9    CDR US ARMY ARDEC  
ATTN AMSTA AR CCH B P DONADIA  
F DONLON P VALENTI  
C KNUTSON G EUSTICE  
K HENRY J MCNABOC  
R SAYER F CHANG  
PICATINNY ARSENAL NJ 07806-5000
- 1    PM ARMS  
ATTN SFAE GCSS ARMS  
BLDG 171  
PICATINNY ARSENAL NJ 07806-5000
- 1    CDR US ARMY ARDEC  
ATTN AMSTA AR WEA J BRESCIA  
PICATINNY ARSENAL NJ 07806-5000
- 1    CDR US ARMY TACOM  
PM COMBAT SYSTEMS  
ATTN SFAE GCS CS  
6501 ELEVEN MILE RD  
WARREN MI 48397-5000
- 1    CDR US ARMY TACOM  
PM SURVIVABLE SYSTEMS  
ATTN SFAE GCSS W GSI H M RYZYI  
6501 ELEVEN MILE RD  
WARREN MI 48397-5000
- 1    CDR US ARMY TACOM  
CHIEF ABRAMS TESTING  
ATTN SFAE GCSS W AB QT  
T KRASKIEWICZ  
6501 ELEVEN MILE RD  
WARREN MI 48397-5000
- 1    COMMANDER  
US ARMY TACOM  
ATTN AMSTA SF  
WARREN MI 48397-5000
- 1    DIR AIR FORCE RSCH LAB  
ATTN MLLMD D MIRACLE  
2230 TENTH ST  
WRIGHT PATTERSON AFB OH 45433-7817
- 1    OFC OF NAVAL RESEARCH  
ATTN J CHRISTODOULOU  
ONR CODE 332  
800 N QUINCY ST  
ARLINGTON VA 22217-5600

NO. OF  
COPIES    ORGANIZATION

- 1    CDR WATERVLIET ARSENAL  
ATTN SMCWV QAE Q B VANINA  
BLDG 44  
WATERVLIET NY 12189-4050
- 2    HQ IOC TANK  
AMMUNITION TEAM  
ATTN AMSIO SMT R CRAWFORD  
W HARRIS  
ROCK ISLAND IL 61299-6000
- 2    COMMANDER  
US ARMY AMCOM  
AVIATION APPLIED TECH DIR  
ATTN J SCHUCK  
FORT EUSTIS VA 23604-5577
- 1    NSWC  
DAHLGREN DIV CODE G06  
DAHLGREN VA 22448
- 2    US ARMY CORPS OF ENGINEERS  
ATTN CERD C T LIU  
CEW ET T TAN  
20 MASSACHUSETTS AVE NW  
WASHINGTON DC 20314
- 1    US ARMY COLD REGIONS  
RSCH & ENGRNG LAB  
ATTN P DUTTA  
72 LYME RD  
HANOVER NH 03755
- 4    CDR US ARMY TACOM  
ATTN AMSTA TR R R MCCLELLAND  
D THOMAS J BENNETT  
D HANSEN  
WARREN MI 48397-5000
- 4    CDR US ARMY TACOM  
ATTN AMSTA JSK S GOODMAN  
J FLORENCE D TEMPLETON  
A SCHUMACHER  
WARREN MI 48397-5000
- 5    CDR US ARMY TACOM  
ATTN AMSTA TR D D OSTBERG  
L HINOJOSA B RAJU  
AMSTA CS SF H HUTCHINSON  
F SCHWARZ  
WARREN MI 48397-5000

NO. OF COPIES	ORGANIZATION
6	BENET LABS ATTN AMSTA AR CCB R FISCELLA M SOJA E KATHE G FRIAR M SCAVULO G SPENCER WATERVLIET NY 12189-4050
4	BENET LABS ATTN AMSTA AR CCB P WHEELER S KRUPSKI J VASILAKIS R HASENBEIN WATERVLIET NY 12189-4050
4	BENET LABS ATTN AMSTA CCB R S SOPOK E HYLAND D CRAYON R DILLON WATERVLIET NY 12189-4050
1	USA SBCCOM PM SOLDIER SPT ATTN AMSSB PM RSS A J CONNORS KANSAS ST NATICK MA 01760-5057
1	NSWC TECH LIBRARY CODE B60 17320 DAHLGREN RD DAHLGREN VA 22448
2	USA SBCCOM MATERIAL SCIENCE TEAM ATTN AMSSB RSS J HERBERT M SENNETT KANSAS ST NATICK MA 01760-5057
2	OFC OF NAVAL RESEARCH ATTN D SIEGEL CODE 351 J KELLY 800 N QUINCY ST ARLINGTON VA 22217-5660
1	NSWC CRANE DIVISION M JOHNSON CODE 20H4 LOUISVILLE KY 40214-5245
2	NSWC ATTN U SORATHIA C WILLIAMS CODE 6551 9500 MACARTHUR BLVD WEST BETHESDA MD 20817

NO. OF COPIES	ORGANIZATION
2	CDR NSWC CARDEROCK DIVISION ATTN R PETERSON CODE 2020 M CRITCHFIELD CODE 1730 BETHESDA MD 20084
4	DIR US ARMY NGIC ATTN D LEITER MS 404 J GASTON MS 301 M HOLTUS MS 301 M WOLFE MS 307 2055 BOULDERS RD CHARLOTTESVILLE VA 22911-8318
4	DIR US ARMY NGIC ATTN S MINGLEDORF MS 504 W GSTATTENBAUER MS 304 R WARNER MS 305 J CRIDER MS 306 2055 BOULDERS RD CHARLOTTESVILLE VA 22911-8318
1	NAVAL SEA SYSTEMS CMD ATTN D LIESE 1333 ISAAC HULL AVE SE 1100 WASHINGTON DC 20376-1100
4	US ARMY SBCCOM SOLDIER SYSTEMS CTR BALLISTICS TEAM ATTN J WARD W ZUKAS P CUNNIFF J SONG KANSAS ST NATICK MA 01760-5019
3	US ARMY SBCCOM SOLDIER SYSTEMS CTR MARINE CORPS TEAM J MACKIEWICZ ATTN AMSSB RCP SS W NYKVIST S BEAUDOIN KANSAS ST NATICK MA 01760-5019
7	US ARMY RESEARCH OFC ATTN A CROWSON H EVERITT J PRATER G ANDERSON D STEPP D KISEROW J CHANG PO BOX 12211 RSCH TRIANGLE PARK NC 27709-2211
1	AFRL MLBC 2941 P ST RM 136 WRIGHT PATTERSON AFB OH 45433-7750

NO. OF  
COPIES    ORGANIZATION

1    DIRECTOR  
LOS ALAMOS NATL LAB  
ATTN F L ADDESSIO T 3 MS 5000  
PO BOX 1633  
LOS ALAMOS NM 87545

4    NSWC  
ATTN J FRANCIS CODE G30  
     D WILSON CODE G32  
     R D COOPER CODE G32  
     J FRAYSSE CODE G33  
DAHLGREN VA 22448

4    NSWC  
ATTN T DURAN CODE G33  
L DE SIMONE CODE G33  
R HUBBARD CODE G33  
DAHLGREN VA 22448

2    AFRL  
ATTN F ABRAMS J BROWN  
BLDG 653  
2977 P ST STE 6  
WRIGHT PATTERSON AFB OH 45433-7739

1    AFRL MLS OL  
ATTN L COULTER  
5851 F AVE  
BLDG 849 RM AD1A  
HILL AFB UT 84056-5713

1    OSD  
JOINT CCD TEST FORCE  
ATTN OSD JCCD R WILLIAMS  
3909 HALLS FERRY RD  
VICKSBURG MS 29180-6199

2    OAK RIDGE NATL LAB  
ATTN R M DAVIS  
     C EBERLE MS 8048  
PO BOX 2008  
OAK RIDGE TN 37831-6195

3    DIR SANDIA NATL LABS  
APPLIED MECHS DEPT  
ATTN MS 9042 J HANDROCK  
     Y R KAN J LAUFFER  
PO BOX 969  
LIVERMORE CA 94551-0969

1    ALLIANT TECHSYSTEMS INC  
4700 NATHAN LN N  
PLYMOUTH MN 55442-2512

NO. OF  
COPIES    ORGANIZATION

5    UNIV OF DELAWARE  
CTR FOR COMPOSITE MTRLs  
ATTN J GILLESPIE M SANTARE  
     S YARLAGADDA S ADVANI  
     D HEIDER  
201 SPENCER LAB  
NEWARK DE 19716

ABERDEEN PROVING GROUND

1    DIRECTOR  
US ARMY RSCH LABORATORY  
ATTN AMSRD ARL CI OK (TECH LIB)  
BLDG 4600

1    US ARMY ATC  
ATTN CSTE DTC AT AC I W C FRAZER  
BLDG 400

1    DIR USARL  
ATTN AMSRD ARL CI  
BLDG

1    DIR USARL  
ATTN AMSRD ARL O AP EG M ADAMSON  
BLDG

1    DIR USARL  
ATTN AMSRD ARL SL BB D BELY  
BLDG 328

2    DIR USARL  
ATTN AMSRD ARL WM J SMITH  
     D LYON  
BLDG 4600

2    DIR USARL  
ATTN AMSRD ARL WM B CHIEF  
     T KOGLER  
BLDG 4600

2    DIR USARL  
ATTN AMSRD ARL WM BC P PLOSTINS  
     J NEWILL  
BLDG 390

3    DIR USARL  
ATTN AMSRD ARL WM BD B FORCH  
     R PESCE-RODRIGUEZ B RICE  
BLDG 4600

3    DIR USARL  
ATTN AMSRD ARL WM BD P CONROY  
     C LEVERITT A ZIELINSKI  
BLDG 390

NO. OF  
COPIES    ORGANIZATION

2    DIR USARL  
      ATTN AMSRD ARL WM BE R LIEB  
          M LEADORE  
      BLDG 4600

1    DIR USARL  
      ATTN AMSRD ARL WM BF  
          S WILKERSON  
      BLDG 390

2    DIR USARL  
      ATTN AMSRD ARL WM M J MCCAULEY  
          S MCKNIGHT  
      BLDG 4600

2    DIR USARL  
      ATTN AMSRD ARL WM MA  
          L GHORSE E WETZEL  
      BLDG 4600

22   DIR USARL  
      ATTN AMSRD ARL WM MB  
          J BENDER T BOGETTI  
          J BROWN L BURTON  
          R CARTER K CHO W DE ROSSET  
          G DEWING R DOWDING  
          W DRYSDALE R EMERSON  
          D GRAY D HOPKINS R KASTE  
          L KECSKES M MINNICINO  
          B POWERS D SNOHA  
          J SOUTH M STAKER  
          J SWAB J TZENG  
      BLDG 4600

11   DIR USARL  
      ATTN AMSRD ARL WM MC J BEATTY  
          R BOSSOLI E CHIN  
          S CORNELISON D GRANVILLE  
          B HART J LASALVIA  
          J MONTGOMERY F PIERCE  
          E RIGAS W SPURGEON  
      BLDG 4600

11   DIR USARL  
      ATTN AMSRD ARL WM MD P DEHMER  
          B CHEESEMAN R DOOLEY  
          G GAZONAS S GHORSE  
          M KLUSEWITZ W ROY J SANDS  
          S WALSH D SPAGNUOLO S WOLF  
      BLDG 4600

2    DIR USARL  
      ATTN AMSRD ARL WM RP J BORNSTEIN  
          C SHOEMAKER  
      BLDG 1121

NO. OF  
COPIES    ORGANIZATION

1    DIR USARL  
      ATTN AMSRD ARL WM T B BURNS  
      BLDG 309

1    DIR USARL  
      ATTN AMSRD ARL WM TA W GILLICH  
      BLDG 309

7    DIR USARL  
      ATTN AMSRD ARL WM TA M BURKINS  
          B GOOCH T HAVEL C HOPPEL  
          E HORWATH J RUNYEON  
          M ZOLTOSKI  
      BLDG 393

1    DIR USARL  
      ATTN AMSRD ARL WM TB P BAKER  
      BLDG 309

1    DIR USARL  
      ATTN AMSRD ARL WM TC R COATES  
      BLDG 309

4    DIR USARL  
      ATTN AMSRD ARL WM TD D DANDEKAR  
          M RAFTENBERG S SCHOENFELD  
          T WEERASOORIYA  
      BLDG 4600

2    DIR USARL  
      ATTN AMSRD ARL WM TE CHIEF  
          J POWELL  
      BLDG 120